F. Pătrulescu[1, 2], T. Groşan[2]

[1] *Tiberiu Popoviciu* Institute of Numerical Analysis
P.O. Box 68-1, 400110 Cluj-Napoca, Romania,

fpatrulescu@ictp.acad.ro

[2]Faculty of Mathematics and Computer Science Babes-Bolyai University, Cluj-Napoca, Romania

Abstract

The steady natural conjugate convection in a long vertical channel filled with a nanofluid and including internal heat generation is presented in this paper. A new mathematical model is proposed for the momentum, energy and nanoparticles' concentration equations. The system of partial differential equations is written in terms of dimensionless velocity, temperature and concentration of the nanoparticles and is solved analytically. The effects of the governing parameters, such as the ratio between the thermophoresis parameter and the Brownian motion parameter, R, and the buoyancy ratio parameter, Nr, on the velocity, temperature and nanoparticles' concentration are studied. It is found that the addition of the nanoparticles into the fluid reduces the temperature and enhances the heat transfer. A limit case when the thermal conductivity of the nanoparticles is much larger than the thermal conductivity of the base fluid has been also studied.

1   Introduction

General fluids used in industrial processes involving heat transfer (energy generation, insulation, cooling of microelectronic components) are water, mineral oil, ethylene glycol, etc. (see [3], [11]). Low values of the physical properties of these fluids (thermal conductivity, density, expansion coefficient, etc.) limit the efficiency of heat transport and it is necessary to obtain new type of fluids, having improved heat transfer characteristics (see [8]). In order to enhance the thermal characteristics of the fluids, one can form mixtures by adding ultra-fine solid particles (metallic, non-metallic or polymeric) to the fluid. Choi [7] was probably, the first one who called the fluids with particles of nanometer dimensions nanofluids.

Over the last twenty years, many industrial processes, biology, medicine, catalytic chemistry and environmental applications started to use nanotechnologies (see [13] and [17]). Different mathematical models were used by several authors to describe heat transfer in nanofluids. Among these models the most used are those where the concentration of nanoparticles is constant and the addition of nanoparticles into the base fluid improved their physical properties (see [18]). Moreover, other models based on physical properties variation include thermal dispersion (see [12]) or Brownian motion (see [14]). A more complex mathematical model (see [4]) considers that nanoparticles' concentration is variable and incorporates the effects of Brownian motion and thermophoresis. Recently, Celli [6] had the idea to combine the model proposed by Buongiorno [4] and the model based on improved physical properties considering for the last one an average concentration of nanoparticles.

Many times theoretical problems as well as industrial processes and natural phenomena are modelled using simple geometries such as infinite channels (see [1], [2]). However, in real simulation it is necessary to take into account the interaction between the convective heat transfer in nanofluid and conductive heat transfer in the thick solid walls. Such situations (i.e. conjugate heat transfer) appears in cellular structures, cavities or channels with solid walls, etc.
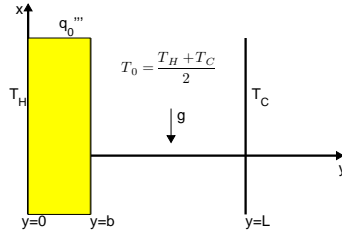
Figure 1: Geometry of the problem and the co-ordinate system

Several authors such as Pătrulescu and Groşan [16], Groşan [9], Groşan and Pop [10] and Li [15] have studied the fully developed flow in a vertical channel filled by a nanofluid using different mathematical models for nanofluid and different boundary conditions. In the present paper, the fully developed conjugate heat transfer in a vertical channel filled with a nanofluid when heat generation in the solid wall is considered has been studied analytically.

2 Notations and preliminaries

Consider the fully developed steady conjugate free convection flow of an incompressible nanofluid in vertical channel differentially heated. The left wall of the channel is kept at a constant temperature T_H, while the right wall has a constant temperature T_C. We consider a two-dimensional coordinate frame in which x-axis is aligned vertically upwards, see Figure 1. The left wall is at $y = 0$ and has thickness b, $b > 0$. The right wall is at $y = L$, $L > b$.

The field variables are the temperature in solid domain T_s, the temperature in nanofluid domain T_f, the velocity $\boldsymbol{v} = (u,\, v)$ and the nanoparticle volume fraction C.

As in [15] it is assumed that the nanoparticles' flux

$$q_c = D_B \nabla C + (D_T/T_f)\, \nabla T_f \tag{1}$$

is zero on the solid vertical walls. In (1) D_B and D_T are the Brownian and thermophoretic diffusion coefficients.

To define the effective viscosity we use a model proposed in [5], namely

$$\mu_{nf} = \frac{\mu_f}{(1 - C_0)^{2.5}}, \tag{2}$$

where μ_f represents the dynamic viscosity of base fluid and C_0 is the reference nanoparticles volume fraction concentration. Moreover, the effective thermal conductivity is approximated by a model introduced in [19], namely

$$k_{nf} = k_f \frac{k_p + 2k_f - 2C_0(k_f - k_p)}{k_p + 2k_f + C_0(k_f - k_p)}, \tag{3}$$

where k_f and k_p are the thermal conductivity of the base fluid and thermal conductivity of the nanoparticles, respectively. The behavior of μ_{nf} and k_{nf} as functions of C_0 was studied in [6] for a side heated square cavity. There, the naofluid is composed of water as base fluid and Alumina as nanoparticles dispersed inside the base fluid.

The limit case of k_{nf} is

$$k_{nf}^{lim} = k_f \frac{1 + 2C_0}{1 - C_0} \tag{4}$$

2

and it is obtained when the ratio k_f/k_p is very small. Physically this is possible when high thermal conductivity nanopraticles such as cooper, gold, carbon nanotubes are used. Thus, it is possible to predict the maximum achievable temperature in this mathematical model for different kind of fluids and concentrations of nanoparticles. Some examples concerning nanofluids' thermo-physical properties are shown in the following table.

Physical properties	Fluid phase (water)	Cu	Al_2O_3	TiO_3
C_p (J/kgK)	4179	385	765	686.2
ρ (kg/m^3)	997.1	8933	3970	4250
k (W/mK)	0.613	400	40	8.9538
$\beta \times 10^{-5}$ (1/K)	21	1.67	0.85	0.9

3 Basic equations

In this section we provide the governing equations for the flow and heat transfer. Thus, as in [16], we consider the following equation for temperature in solid domain

$$\alpha_s \nabla^2 T_s + \frac{q_0'''}{(\rho c)_s} = 0, \tag{5}$$

where q_0''' represents the heat generation, α_s is the thermal diffusivity coefficient and $(\rho c)_s$ represents the heat capacity. As in [10], in the fluid domain we consider the following four field equations in the vectorial form. More exactly, the equations embody the conservation of total mass, momentum, thermal energy and nanoparticles' concentration. Thus, we have

$$\nabla \cdot \boldsymbol{v} = 0, \tag{6}$$

$$
\begin{aligned}
\rho_f(\boldsymbol{v} \cdot \nabla \boldsymbol{v}) \quad = \quad & \mu_{nf} \nabla^2 \boldsymbol{v} \\
& + \{\rho_p C + (1 - C)[\rho_f(1 - \beta(T_f - T_0))]\}\boldsymbol{g},
\end{aligned}
\tag{7}
$$

$$(\rho c)_f(\boldsymbol{v} \cdot \nabla T_f) = k_{nf}\nabla^2 T_f + (\rho c)_p[D_B \nabla T_f \cdot \nabla C + (D_T/T_f)\nabla T_f \cdot \nabla T_f], \tag{8}$$

$$\boldsymbol{v} \cdot \nabla C = \nabla(D_B \nabla C + (D_T/T_f)\nabla T_f). \tag{9}$$

Here ρ_f is the fluid density, ρ_p is the nanoparticle mass density, β represents the thermal expansion coefficient, $\boldsymbol{g}$ is the gravitational acceleration. Finally, $(\rho c)_f$ and $(\rho c)_p$ are the heat capacity of the base fluid and of the nanoparticle material, respectively.

In the rest of the paper we use the following linearized version of the momentum equation (see [10])

$$
\begin{aligned}
\rho_f(\boldsymbol{v} \cdot \nabla \boldsymbol{v}) \quad = \quad & \mu_{nf}\nabla^2 \boldsymbol{v} + [(\rho_p - \rho_{f_0})(C - C_0) \\
& - (1 - C_0)\rho_{f_0}\beta(T_f - T_0)]\boldsymbol{g},
\end{aligned}
\tag{10}
$$

where ρ_{f_0} represents the reference fluid density.

Based on the fact that the flow is fully developed we introduce the following assumptions

$$v = 0, \ \frac{\partial T_f}{\partial x} = 0, \ \frac{\partial T_s}{\partial x} = 0, \ \frac{\partial C}{\partial x} = 0. \tag{11}$$

Taking into account (1) and (11) the governing equations for the flow and heat transfer (5)–(10) become

$$\alpha_s \frac{d^2 T_s}{dy^2} + \frac{q_0'''}{(\rho c)_s} = 0, \tag{12}$$

$$\frac{d^2 T_f}{dy^2} = 0, \tag{13}$$

$$D_B \frac{dC}{dy} + \frac{D_T}{T_f}\frac{dT_f}{dy} = 0, \tag{14}$$

$$\mu_{nf}\frac{d^2 u}{dy^2} + (1 - C_0)\rho_{f_0}\beta(T_f - T_0)g - (\rho_p - \rho_{f_0})(C - C_0)g = 0, \tag{15}$$

subject to the boundary conditions

$$T_s|_{y=0} = T_H, \quad T_f|_{y=L} = T_C, \tag{16}$$

$$T_f|_{y=b} = T_s|_{y=b}, \tag{17}$$

$$k_s \frac{dT_s}{dy}|_{y=b} = k_{nf} \frac{dT_f}{dy}|_{y=b}, \tag{18}$$

$$u(b) = u(L) = 0. \tag{19}$$

In (18) k_s denotes the thermal conductivity of solid domain. To complete the set of equations and boundary conditions we add the following nanoparticles' conservation relation

$$\int_b^L C(y)\,dy = Q_0, \tag{20}$$

where Q_0 is defined in the next section.

4 Dimensionless Equations

In this section we solve equations (12)–(15) subject to (16)–(20). To this end, we consider the following dimensionless variables used in [16].

$$Y = \frac{y}{L}, \; \Theta_s = \frac{k_s(T_s - T_0)}{q_0''' L^2}, \; \Theta_f = \frac{k_s(T_f - T_0)}{q_0''' L^2}, \; \phi = \frac{C - C_0}{C_0}, \; U = \frac{u}{U_c}, \tag{21}$$

where U_c is the characteristic velocity given by

$$U_c = \frac{g\beta(\frac{q_0''' L^2}{k_s})L^2}{\nu_f}. \tag{22}$$

In (22) ν_f represents the kinematic viscosity of base fluid.

We substitute dimensionless variables (21) into equations (12)–(15) and we obtain the following ordinary differential equations

$$\frac{d^2\Theta_s}{dY^2} + 1 = 0, \tag{23}$$

$$\frac{d^2\Theta_f}{dY^2} = 0, \tag{24}$$

$$\frac{d\phi}{dY} + \frac{R}{w\Theta_f + 1}\frac{d\Theta_f}{dY} = 0, \tag{25}$$

$$\frac{d^2U}{dY^2} = N_r(1 - C_0)^{2.5}\phi - (1 - C_0)^{3.5}\Theta_f, \tag{26}$$

where w is a dimensionless constant given by

$$w = \frac{q_0''' L^2}{k_s T_0} = \frac{2q_0''' L^2}{k_s(T_H + T_C)} \tag{27}$$

and, as in [10], Nr is the buoyancy ratio parameter defined by

$$Nr = \frac{g(\rho_p - \rho_{f_0})C_0 L^2}{\mu_f U_c}. \tag{28}$$

Moreover, R is given by

$$R = \frac{N_t}{N_b}, \tag{29}$$

4

and it represents the ration between the thermophoresis parameter and the Brownian motion parameter (see [10]).

The boundary conditions (16)–(19) become

$$\Theta_s|_{Y=0} = q, \tag{30}$$

$$\Theta_s|_{Y=r} = \Theta_f|_{Y=r}, \tag{31}$$

$$\frac{d\Theta_s}{dY}|_{Y=r} = K\frac{d\Theta_f}{dY}|_{Y=r}, \tag{32}$$

$$\Theta_f|_{Y=1} = -q, \tag{33}$$

$$U(r) = U(1) = 0, \tag{34}$$

where r, q, K are given by

$$r = \frac{b}{L}, \quad q = \frac{k_s(T_H - T_C)}{2q_0''' L^2}, \quad K = \frac{k_{nf}}{k_s}. \tag{35}$$

Finally, we choose $Q_0 = C_0 L(1 - r)$ such that (20) takes the form

$$\int_r^1 \phi(Y)dY = 0. \tag{36}$$

5   Results and discussions

In this section we determine the exact solutions of equations (23)–(26) and discuss the results. Integrating equations (23), (24) and taking into account boundary conditions (30)–(33) we obtain

$$\Theta_s(Y) = -\frac{Y^2}{2} + A_1 Y + A_2, \tag{37}$$

and

$$\Theta_f(Y) = A_3 Y + A_4. \tag{38}$$

The constants A_1, A_2, A_3, A_4 are given by

$$A_1 = r + K\frac{\frac{1}{2}r^2 + 2q}{r(1 - K) - 1}, \quad A_2 = q, \tag{39}$$

and

$$A_3 = \frac{\frac{1}{2}r^2 + 2q}{r(1 - K) - 1}, \quad A_4 = -q - A_3. \tag{40}$$

Moreover, integrating (25) and taking into account (38), (40) and (36) we obtain

$$\phi(Y) = -\frac{R}{w}\left(\ln(wA_3 Y + wA_4 + 1) - \frac{\mathcal{C}_a}{1 - r}\right). \tag{41}$$

The constant $\mathcal{C}_a$ is given by

$$\mathcal{C}_a = (1 + z)\ln(wA_3 + wA_4 + 1) - (r + z)\ln(wA_3 r + wA_4 + 1) - (1 - r),$$

where

$$z = \frac{1 + wA_4}{wA_3}.$$

Finally, integrating (26) and taking into account (38), (40), (41) and boundary conditions (34) we obtain

$$U(Y) = G(Y) + \mathcal{C}_1 Y + \mathcal{C}_2. \tag{42}$$

5

The constants $\mathcal{C}_1$, $\mathcal{C}_2$ are given by

$$\mathcal{C}_1 = \frac{G(r) - G(1)}{1 - r}, \quad \mathcal{C}_2 = \frac{rG(1) - G(r)}{1 - r}, \tag{43}$$

and function G is defined in the following way

$$G(Y) = (1 - C_0)^{2.5}\left[-\mathcal{C}_b\left(\frac{Y^2}{2} + zY + \frac{z^2}{2}\right)\ln(wA_3Y + wA_4 + 1)\right.$$

$$\left.-(1 - C_0)A_3\frac{Y^3}{6} + \left(\frac{3}{2}\mathcal{C}_b + \frac{\mathcal{C}_a\mathcal{C}_b}{1 - r} - (1 - C_0)A_4\right)\frac{Y^2}{2} + z\mathcal{C}_b\frac{Y}{2}\right],$$

where

$$\mathcal{C}_b = \frac{RN_r}{w}.$$

Next we determine the Nusselt number. For the conjugate wall is defined as:

$$Nu = \frac{hL}{k_f}|_{y=b}, \tag{44}$$

where the convective heat transfer coefficient, h, is obtained from relation (see [16]):

$$-k_{nf}\frac{dT_f}{dy}|_{y=b} = h(T_f|_{y=b} - T_0). \tag{45}$$

Substituting (45) in (44) the dimensionless form of Nusselt number becomes:

$$Nu = -\frac{k_{nf}}{k_f}\frac{1}{\Theta_f|_{Y=r}}\frac{d\Theta_f}{dY}|_{Y=r}. \tag{46}$$

Tacking into account (38) we deduce that

$$Nu = -K\frac{A_3}{A_3r + A_4}. \tag{47}$$

Finally, we present the effects of the governing parameters on the velocity, temperature and nanoparticles' concentration. In this study we consider the following fixed values $r = 0.3$, $T_H = 300$, $T_C = 15$, $k_s = 1.2$, $k_f = 0.613$, $C_0 = 0.08$, $q = 1$. Figure 2 presents the variation of the solid temperature profiles for different kind of nanoparticles. It is obvious that the addition of the nanoparticles leads to a decrease of the temperature in solid, specially on the solid-fluid interface and the results for copper nanoparticles are the most close to the limit case. The influence of the parameter R on the nanoparticles' concentration profiles in the limit case is depicted in Figure 3. The concentration profile is almost flat for small values of the parameter R, while for large values large differences between the concentration values on the left and on the right walls appear. The variation of the velocity profiles with R and Nr is given in Figures 4 and 5, respectively. In both cases there is a reversed flow near the right wall. The maximum velocity increases with the increase of R and Nr, respectively.

Acknowledgement

References

[1] AUNG, W., WORKU, G., *Theory of fully developed, combined convection including flow reversal*, ASME J. Heat Transfer, **108** (1986), 485–488.
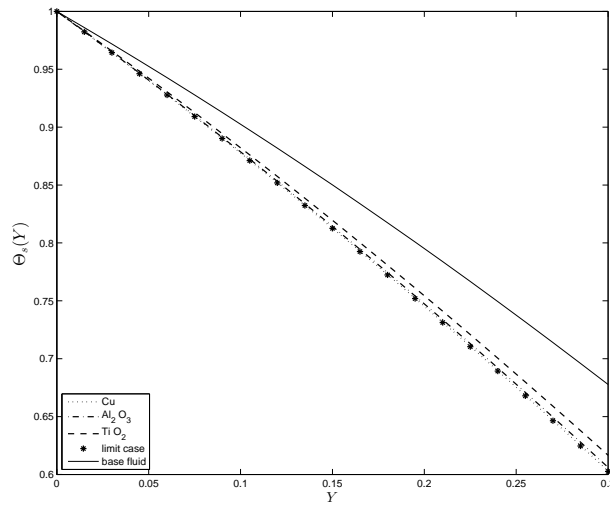
Figure 2: Solid temperature

[2] BARLETTA, A., *Analysis of combined forced and free flow in a vertical channel with viscous dissipation and isothermal-isoflux boundary conditions*, ASME J. Heat Transfer, **121** (1999), 349–356.

[3] BEJAN, A., *Convection Heat Transfer (2nd ed.)*, Wiley, New York, 1995.

[4] BUONGIORNO, J., *Convective transport in nanofluids*, Journal of Heat Transfer, **128** (2005), no. 3, 240–250.

[5] BRINKMAN, H.C., *The viscosity of concentrated suspensions and solutions*, J. Chem. Phys., **20** (1952), 571–581.

[6] CELLI, M., *Non-homogeneous model for a side heated square cavity filled with a nanofluid*, International Journal of Heat and Fluid Flow, **44** (2013), 327–335.

[7] CHOI, S.U.S., *Enhancing thermal conductivity of fluids with nanoparticles*, ASME FED, **231** (1995), 99–103.

[8] DAUNGTHONG, W., WONGWISES, S., *A critical review of convective heat transfer of nanofluids*, Renewable and Sustainable Energy Reviews, **11** (2007), 797–817.

[9] GROŞAN, T., *Thermal dispersion effect on fully developed free convection of nanofluids in a vertical channel*, Sains Malaysiana, **40** (2011), 1429–1435.

[10] GROŞAN, T., POP, I., *Fully developed mixed convection in a vertical channel filled by a nanofluid*, Journal of Heat Transfer, **134** (2012), no. 8, 082501-082501-5.

[11] INGHAM, D.B., POP, I., *Transport in Porous Media*, vol. 1, 2 and 3, Elsevier, 1998, 2002, 2005.

[12] KHANAFER, K., VAFAI, K., LIGHTSTONE, M., *Buoyancy-driven heat transfer enhancement in a two-dimensional enclosure utilizing nanofluids*, Int. J. Heat Mass Transfer, **46** (2003), 3639–3653.

[13] KLEINSTRAUER, C., *Microfluidics and Nanofluidics. Theory and Selected Applications*, Wiley, New Jersey, 2013.

[14] KOO, J., KLEINSTREUER, C., *Laminar nanofluid flow in microheat-sinks*, Int. J. Heat Mass Transfer, **48** (2005), 2652–2661.
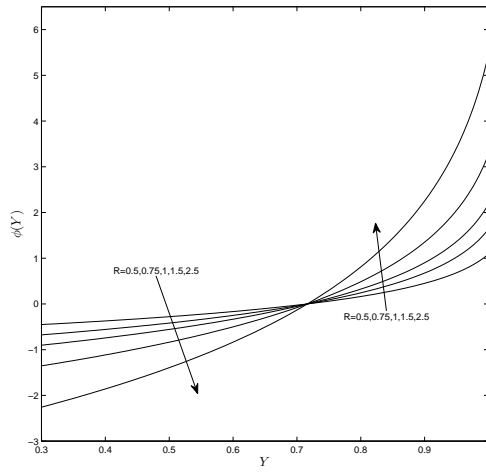
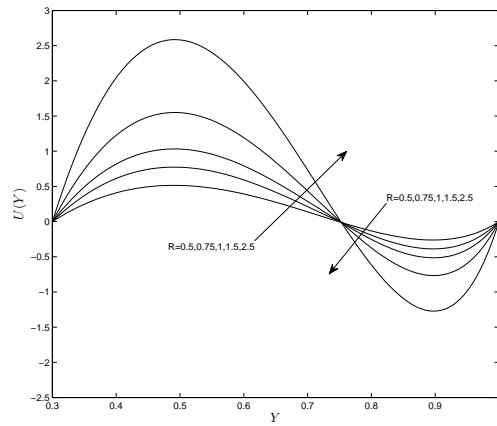Figure 3: Nanoparticles' concentration

Figure 4: Velocity profile, $N_r = 100$

[15] Lı, W., *Exact solutions for free convective heat transfer in nanofluids in a vertical channel*, Open Journal of Heat, Mass and Momentum Transfer (HMMT), **1** (2013), 19–34.

[16] PĂTRULESCU, F. and GROȘAN, T., *Conjugate heat transfer in a vertical channel filled with a nanofluid adjacent to a heat generating solid domain*, Rev. Anal. Numér. Théor. Approx., **36** (2010) no. 1, 141–149.

[17] SCHAFER, H.-E., *Nanoscience. The Science of the Small in Physics, Engineering, Chemistry, Biology and Medicine*, Springer, Heidelberg, 2010.

[18] TIWARI, R.K., DAS, M.K., *Heat transfer augmentation in a two sided lid-driven differentially heated square cavity utilizing nanofluids*, Int. J. Heat Mass Transfer, **50** (2007), 2002–2018.

[19] WANG, X.Q., MUJUMDAR, A.S., *A review on nanofluids-part I: Theoretical and numerical investigations*, Brazilian Journal Of Chemical Engineering, **25** (2008), 613–630.
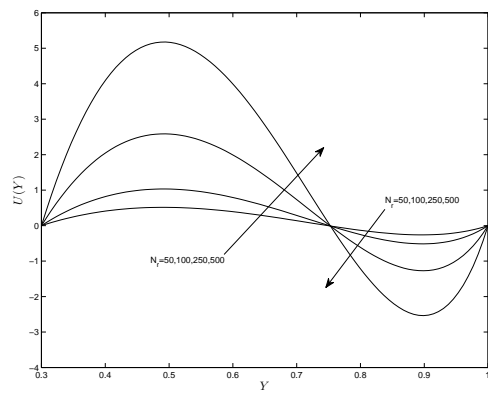
Figure 5: Velocity profile, $R = 1$